Transitions and distribution functions for chaotic systems

Shau-Jin Chang and Jon Wright
Physics Department, University of Illinois at Urbana-Champaign, Urbana, Illinois 61801
(Received 22 September 1980)

We study chaotic systems generated by deterministic or probablistic mappings. We introduce the density function which is an eigenfunction of a probability-preserving kernel K. We are able to show that all eigenvalues of K have magnitude less than or equal to 1 and that the only magnitude-one eigenvalues are the Nth roots of unity. We have also calculated the corresponding eigenfunctions associated with these magnitude-one eigenvalues: These eigenfunctions can be expanded in terms of N positive functions having disjoint support. We then concentrate on a one-dimensional system, and study the behavior and mechanism for various chaotic transitions. We find that the mechanism associated with the 2 to 1 (or more generally, $2N$ to N) transition is different from those associated with other chaotic transitions. We then determine the conditions for these transitions, and express them in a universal form. We confirm the Huberman-Rudnick scaling in the large 2^n to 2^{n-1} chaotic-transition region, and determine the prefactor at these transitions. In addition, we establish a simple relation between the Lyapunov exponent and the folding of the distribution functions. We have also studied the chaotic regions of this system numerically.

I. INTRODUCTION

The problem of chaotic behavior in deterministic nonlinear systems has received considerable attention in recent years.[1-5] In particular one-dimensional maps have been extensively studied as there is increasing evidence that under certain circumstances complicated systems have an underlying one-dimensional structure. For a recent review of one-dimensional maps see the article by May.[1] The features of interest are the sequences of bifurcations leading to 2^n cycles of the basic periods and the subsequent chaotic behavior which has a similar bifurcation structure. All sequences of bifurcations occur as some parameter is changed. Smaller and smaller changes of the parameter lead to limit cycles with larger n. Finally an accumulation point is reached and for values of the parameter beyond that point the process is inverted, except that the behavior is now characterized by cycling between regions instead of isolated points. These sequences of bifurcations are characterized by a remarkable scaling property discovered by Feigenbaum.[2] He discusses the scaling for the isolated fixed points. Huberman and Rudnick[3] point out that the same scaling behavior applies in the chaotic region as well. The original purpose of this investigation was to investigate what changes in the theory result if the mapping is allowed to be slightly probabilistic. Some information on this point is discussed by Crutchfield and Huberman.[4] The theory we developed turned out to provide us with some new insights into the deterministic one-dimensional map, and consequently part of this paper discusses those developments.

It seems appropriate to study some of the properties of stochastic maps, and eventually to be more precise about the sources and size of the stochasticity as related to some experimental configuration. In this paper we set up a formalism for discussing the equilibrium-density distribution and the approach to equilibrium. In the next section we will describe the formalism and demonstrate certain general properties of a wide class of models. Then in the third section we will restrict ourselves to a deterministic one-dimensional map and we will exhibit a number of simple features of such maps. We discuss the transitions between 2^n cycles and 2^{n-1} cycles and then the new behavior that occurs in the three to one transition. In the large 2^n to 2^{n-1} chaotic-transition region, we confirm the Huberman-Rudnick scaling[3] and are able to determine the prefactor associated with these chaotic transitions. Some other simple scaling properties are discussed as well. A simple expression for the divergence of neighboring points (Lyapunov exponents) is given in Sec. IV. The numerical method used is discussed briefly in Appendix A.

II. GENERAL THEORY

We consider the maps of the unit interval onto itself by a probability-conserving mapping,

$$\psi(x)=\int_0^1 K(x,y)\phi(y)dy\,, \tag{2.1}$$

where

$$\int_0^1 K(x,y)dx=1 \tag{2.2}$$

and

$$K(x,y)\geq 0\,. \tag{2.3}$$

For a technical reason, basically aimed at ruling out general unitary kernels associated with area-preserving mappings, we also need the operator K to have an additional property known to mathematicians as quasicompact. Equation (2.2) immediately gives

$$\int_0^1 \psi(x)dx = \int_0^1 \phi(x)dx . \tag{2.4}$$

A surprising amount of information can be obtained from the conditions (2.2) and (2.3). In particular we will show that the equilibrium distribution is characterized by N ($N=1,2,3\ldots,$) disjoint regions all having the same area. The operator K maps cyclically the function characterizing one of these regions into the function for another region. These statements (with some qualifications) are independent of the dimensionality of the system. Note that the operator in (2.1) can correspond to a set of differential equations with no time-dependent parameters or to a set with periodic parameters. The mapping would then be for a fixed time interval. For our numerical examples we will use

$$x_{n+1} = \lambda x_n(1-x_n) \tag{2.5}$$

which gives for K,

$$K(x,y) = \delta[x - \lambda y(1-y)] . \tag{2.6}$$

One way to introduce probabilistic behavior is to assume that at each iteration λ is chosen according to a probability distribution $P(\lambda)$. Then we would have for K,

$$K(x,y) = \int_0^4 d\lambda\, P(\lambda)\delta[x - \lambda y(1-y)] .$$

A simple version of this is to take K to be the sum of two terms

$$K(x,y) = p\delta[x - \lambda_1 y(1-y)] + (1-p)\delta[x - \lambda_2 y(1-y)] . \tag{2.7}$$

Note that this mechanism for adding probabilistic behavior is different from the one studied in Ref. 4. To study the solutions to Eq. (2.1), we will imagine finding the eigenvalues and eigenfunctions of K. We suppose that K is reasonably well behaved, although operators such as the one in Eq. (2.6), are acceptable provided we allow δ-function distributions. The stable periodic cycles correspond to δ-function eigenfunctions. The eigenfunction problem for K involves finding both left and right eigenfunctions

$$\int_0^1 K(x,y)R(y)dy = \eta R(x) \tag{2.8}$$

and

$$\int_0^1 L(x)K(x,y)dx = \eta L(y) . \tag{2.9}$$

By integrating Eq. (2.8) and using Eq. (2.2) we see that if $\eta \neq 1$,

$$\int_0^1 R(x)dx = 0 .$$

Next take the absolute value of Eq. (2.8) to obtain

$$\int_0^1 K(x,y)\,|R(y)|\,dy \geq |\eta|\;|R(x)| . \tag{2.10}$$

We now have the following results:

Lemma 1: All eigenvalues η of K satisfy

$$|\eta| \leq 1 .$$

This result follows immediately from integrating Eq. (2.10) over x.

Lemma 2: If $R(x)$ is a right eigenfunction of K with eigenvalue $|\eta| = 1$, then $\phi_0(x) \equiv |R(x)|$ is an eigenfunction with eigenvalue 1.

Proof. From Eq. (2.10) and the fact that $|\eta| = 1$ we have

$$D(x) \equiv \int_0^1 K(x,y)\phi_0(y)dy - \phi_0(x) \geq 0 .$$

Integrating $D(x)$ over x and using Eq. (2.2), we have

$$\int_0^1 D(x)dx = 0 .$$

This implies $D(x) = 0$, and consequently

$$K\phi_0 = \phi_0 .$$

Lemma 3: If ϕ is an eigenfunction of K with eigenvalue $|\eta| = 1$, and if there is no degeneracy for the eigenvalue 1, we have

(a) There is an integer N such that $\eta^N = 1$. This says that all eigenvalues of absolute value 1 are Nth roots of unity.

(b) There are N nonnegative functions χ_j with disjoint support such that

$$K\chi_j = \chi_{j+1}, \quad j = 1,2,\ldots,N-1$$

and

$$\chi_{N+1} = \chi_1 .$$

(c)

$$\phi_0(x) = \sum_{j=1}^{N} \chi_j(x) .$$

(d) There are N eigenfunctions of K having eigenvalues with absolute value 1. Define $\alpha = e^{-2\pi i/N}$.

They are (in addition to ϕ_0)

$$\phi_l(x)=\sum_{k=1}^{N}\alpha^{kl}\chi_k(x).$$

Note that this implies that the support of ϕ_l separates into N disjoint regions and that within each region $\phi_l(x)/|\phi_l(x)|$ is a constant phase. Also each Nth root of unity is represented once and only once.

Proof. Suppose

$$\int K(x,y)\phi(y)dy=\eta\phi(x)$$

with

$$|\eta|=1.$$

Since K is real, ϕ^* and η^* satisfy a similar equation. From Lemma 1 we have

$$K|\phi|=|\phi|$$

with

$$\phi_0(x)=|\phi(x)|.$$

Notice that ϕ and ϕ_0 have the same region of support. We consider the ratio $\phi(x)/\phi_0(x)$ which is obviously a phase $e^{i\theta(x)}$ and define the ratio to be 1 where $\phi_0(x)=0$ (the region where $\phi_0=0$ is irrelevant). We introduce the expression

$$\int_0^1 dx\int_0^1 dy\,\phi_0(y)\left(\frac{\phi(x)}{\phi_0(x)}-\eta^*\frac{\phi(y)}{\phi_0(y)}\right)\left(\frac{\phi^*(x)}{\phi_0(x)}-\eta\frac{\phi^*(y)}{\phi_0(y)}\right)K(x,y)=(1-\eta\eta^*)\int dx\frac{\phi(x)\phi^*(x)}{\phi_0(x)}=0.$$

Since the integrand is nonnegative, if $K(x,y)\neq 0$, then

$$\frac{\phi(x)}{\phi_0(x)}-\eta^*\frac{\phi(y)}{\phi_0(y)}=0. \tag{2.11}$$

We will demonstrate that the support of ϕ(or ϕ_0) is made up of disjoint regions and that in each region ϕ and ϕ_0 differ by a constant phase (different for each region).

Definition of region. Consider only the points in the support of ϕ_0. Points x_1, x_2 (or y_1, y_2) are in the same region if any of the following conditions is satisfied: (a) y_1 and y_2 are in the same region if there exists an x such that $K(x,y_1)\neq 0$, and $K(x,y_2)\neq 0$. (b) x_1 and x_2 are in the same region if there exists a y such that $K(x_1,y)\neq 0$ and $K(x_2,y)\neq 0$. (c) x_1 and x_2 are in the same region if there exists an x_3 such that (x_1,x_3) are in a region and (x_2,x_3) are in a region. Similarly for y.

From Eq. (2.11) it is clear that $\phi(y)/\phi_0(y)$ has the same phase in a region, and that the phase in regions related by $K(x,y)\neq 0$ is

$$\frac{\phi(y)}{\phi_0(y)}=\eta\frac{\phi(x)}{\phi_0(x)}. \tag{2.12}$$

We now consider an infinitesimal neighborhood in the support of ϕ containing a point x. We now follow this neighborhood under iterations of K. If it returns after N iterations to partially overlap the original neighborhood, the phase must be restored to its original value and by using Eq. (2.12) N times,

$$\frac{\phi(x)}{\phi_0(x)}=\eta^N\frac{\phi(x)}{\phi_0(x)},$$

or

$$\eta^N=1. \tag{2.13}$$

Clearly if there is any finite width to the mapping, then the neighborhood must return after a finite number of iterations provided that the space is finite. This is true in any number of dimensions. As the width of K gets narrower, larger N values are permitted, but the maximum N is related to the width of K. This establishes part (a) of the Lemma.

We define χ_j to be ϕ_0 on the jth region, i.e.,

$$\chi_j=\begin{cases}\phi_0, & x\in j\text{th region}\\ 0, & \text{otherwise}\end{cases}$$

since K connects ϕ_0 in the jth region to ϕ_0 in the $(j+1)$th region, we have

$$K\chi_j=\chi_{j+1}$$

as desired; parts (b) and (c) then follow. Knowing χ_j, we can verify easily that $\phi_l(x)$ is indeed the eigenfunction of K with eigenvalue $\eta=\exp(i2\pi l/N)$:

$$\begin{aligned}K\phi_l&=\sum_k a^{kl}K\chi_k\\&=\sum_k a^{kl}\chi_{k+1}\\&=a^{-l}\sum_k a^{kl}\chi_k\\&=e^{i2\pi l/N}\phi_l.\end{aligned}$$

This completes the proof of Lemma 3. For an alternate proof of part (b), see Appendix B.

We wish to comment about the special case in which the width of K is zero. This case includes the iterations of difference equations of the form

$$x_{N+1} = f(x_N)$$

with

$$K(x, y) = \delta[x - f(y)] .$$

Since the mapping is from a point of zero width to another point of zero width, the iteration of a point may never return to itself. However, in the chaotic region a small neighborhood will return and cover the original neighborhood after a sufficient number of iterations. If we assume that the phase of the function $\phi(x)$ is piecewise continuous, then it is possible to establish Lemma 3 even with a δ-function K. We shall modify our definition of regions by assuming that there are small neighborhoods which lie entirely inside these regions. Finally we can show that if the eigenvalue equal to one is degenerate then there will be disjoint groups mapping onto themselves, but not onto members of other groups and there will be one such group for each eigenvalue equal to unity. For a general mathematical discussion of some of the above ideas, see Ref. 6.

We have computed some eigenvalues and eigenfunctions of K. An example of an eight cycle is shown in Fig. 1 for the K of Eq. (2.6). In later sections we will show more examples of the distribution function, paying particular attention to transition regions. An important feature of Fig. 1 is the narrowness of most of the regions (they all have equal area under the curve). In an experimental setting it would be difficult to distinguish a chaotic eight cycle from an eight cycle with δ-function supports. They will both have an underlying periodicity which will give similar results in experiments such as the one Feigenbaum[2] discusses.

The effect of adding some randomness to the system is illustrated in Figs. 2 and 3. In Fig. 2 we added a very small extra term to the K that gave Fig. 1. In the notation of Eq. (2.7) we chose $p = 0.95$, $\lambda_1 = 3.571$, and $\lambda_2 = 3.5$, the latter value corresponding to periodic cycles. The small amount of random behavior changed the eight-cycle regions of Fig. 1 into the two-cycle regions of Fig. 2. Chaos also results if two periodic maps are added together. We choose two λ's, each of them corresponding to a periodic two cycle and added the maps according to Eq. (2.7). The resulting chaotic behavior is shown in Fig. 3.

We wish to mention here the general behavior of the eigenfunctions. If K is bounded and piecewise continuous, the eigenfunction ϕ will at least be piecewise continuous. For a deterministic system $x_{n+1} = f(x_n)$, $K(x, y)$ is given by

$$K(x, y) = \delta[x - f(y)].$$

The eigenfunction is either a sum of δ functions or an ill-behaved function ϕ. In the latter case, if the maximum of $f(x)$ is quadratic, ϕ will in general consist of an infinite number of square-root singularities of the form $c_i/(|x - x_i|)^{1/2}$. The function ϕ is integrable, but not continuous, nor bounded. However, the phase of ϕ is usually continuous. In our figures we have cut off the highest of the peaks that survive the numerical approxima-

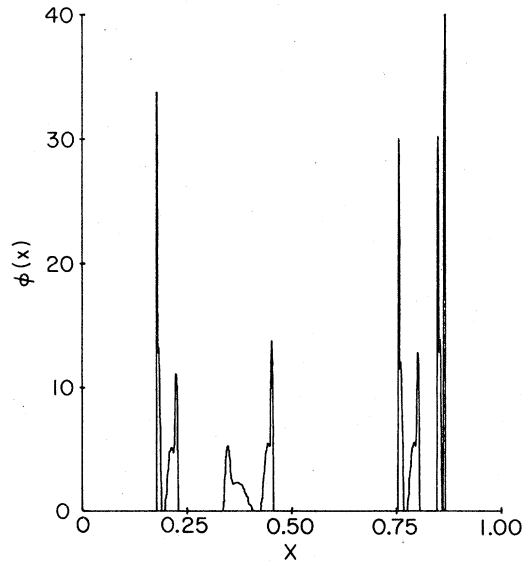

FIG. 1. A chaotic eight cycle, K given by (2.6) with $\lambda = 3.571$. Note that due to numerical errors introduced in approximating a δ function all of the couplings are only approximate.

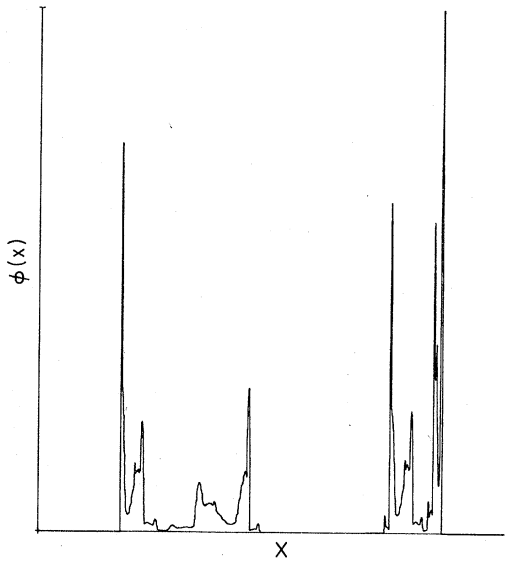

FIG. 2. A small second term has been added to the K of Fig. 1 to simulate noise. K is given by (2.7) with $\lambda_1 = 3.571$, $\lambda_2 = 3.5$, and $p = 0.95$.

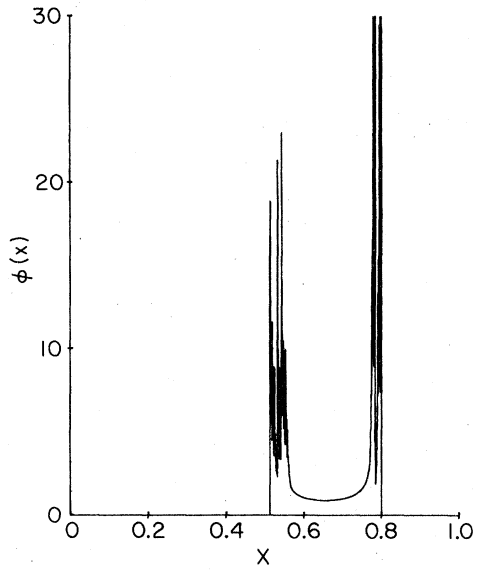

FIG. 3. K given by (2.7) with $p=0.5$, $\lambda_1=3.2$, $\lambda_2=3.13$ $=3.136$.

tion so that more detail can be seen. Since we only have finite resolution, the ϕ that we observed is the average of ϕ over finite bins. This will smooth out both the δ functions and the square-root singularities. Hence, we cannot distinguish numerically whether the system is periodic with a large period or is aperiodic.

We now discuss the approach of a distribution to the equilibrium distribution. Imagine expanding K in terms of its eigenfunctions to obtain

$$K \sim \sum_m \eta_m \frac{|\psi_m\rangle\langle\phi_m|}{\langle\phi_m|\psi_m\rangle} .$$

The Nth iterates of K on an arbitrary initial distribution is given by

$$K^N \sim \sum_m (\eta_m)^N \frac{|\psi_m\rangle\langle\phi_m|}{\langle\phi_m|\psi_m\rangle} . \tag{2.14}$$

It is evident that the eigenvalues having magnitudes nearest to unity are dominant in determining the approach to equilibrium. As some parameter in K is changed, the eigenvalues change and at a bifurcation the number of eigenvalues of modulus unity changes. For instance, at the transition from a four cycle to a two cycle, two of the eigenvalues change from $\pm i$ to complex numbers with magnitude less than one. For the K of Eq. (2.6) it is possible to discuss a scaling behavior of the eigenvalues at a transition. We do this in Sec. V. In the next section we discuss the changes the distribution function undergoes during a transition.

III. TRANSITIONS IN THE CHAOTIC REGION

As we increase the parameter λ in a typical deterministic system such as Eq. (2.5) beyond a critical λ_c, we find that there are many disjoint chaotic regions. As λ increases, the disjoint regions start to merge and finally become one region.[5] In addition to the gross features described above, higher-order cycles and chaotic processes also appear and disappear at intermediate values of λ. These finer structures can be described separately. In the following we shall describe the mechanisms that lead to the merging of disjoint chaotic regions.

In Sec. II we demonstrated that the presence of N disjoint regions is related to the existence of eigenstates with eigenvalues η obeying $\eta^N=1$. These disjoint regions are linked to each other under the operation of K. As we vary λ, the disjoint regions may combine. This happens in two natural ways. In the first case (see Figs. 4 and 5) as λ changes the boundaries of the disjoint regions (here B and C of Fig. 4) move toward each other and finally B and C become the same point. Define region I to be the line segment $I=(A,B)$ and region II$=(C,D)$. Since all points in region I map into II and vice versa their intersection point $(B$-$C)$ must be an unstable fixed point.

In the second way of merging, the disjoint regions never overlap. However, as λ reaches the transition value, the density $\phi(x)$ in the gaps starts to develop a nonvanishing value. An example of this is shown in Figs. 6–8. Thus we could achieve a single region by filling in the gaps between the

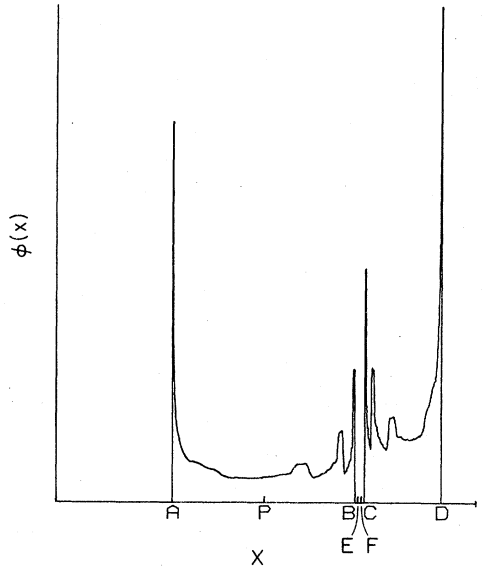

FIG. 4. A chaotic two cycle just before the transition to a single region. K given by (2.6) with $\lambda=3.67$.

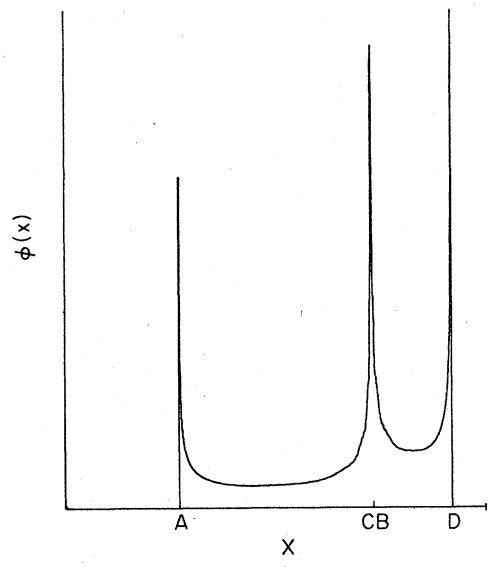

FIG. 5. Just past the transition from 2 to 1, $\lambda = 3.679$.

originally separated regions. As we shall see, both mechanisms are realized for Eq. (2.5). We present an example of each mechanism:

1. 2^n to 2^{n-1} merging. We first consider the $2 \to 1$ merging. We can extend our result trivially to cover the more general 2^n to 2^{n-1} case. In the transition from two chaotic regions to a single chaotic region, we encounter the first mechanism discussed above. Denote the position of the maximum of $f(x)$ by P. The peak position is mapped in subsequent interactions as follows:

$$f\colon\ P \to \text{point } D \to \text{point } A \to \text{point } C \to \text{point } B \to \text{interior of } CD .$$

The points are shown in Fig. 4. It is important that P lies in the interior of AB and that point B folds into the interior of AP during the mapping. We can easily see that region AB is mapped into CD and vice versa. In the gap BC there are two special points E, F (see Fig. 4). F is an unstable fixed point lying inside the gap BC and E is the otherpoint such that $f(E) = C$. During an iteration, points inside the line segment BE are mapped into the interior of CD and are removed from the gap BC. Under repeated iterations all points in the gap are gradually moved into the segment BE and then removed from the gap. It is easy to see that points to the left of point A and to the right of point B are also mapped into regions AB and CD after repeated iterations. As we increase the coupling constant λ, points B and C move toward F. At the transition coupling λ_1, points B, C, and F all coincide and the two regions become linked. For $\lambda > \lambda_1$, regions AB and CD become overlapped at CB and we have only one region as shown in Fig. 5. The requirement that $f^3(P)$ is a fixed point determines the transition value of λ. Thus we have

$$f^{(3)}(P) = f^4(P) . \tag{3.1}$$

In terms of $F(x) = f^2(x)$ we can reexpress this as

$$F^3(P) = F^2(P) \neq F(P) . \tag{3.2}$$

As we shall see this equation applies for both transition mechanisms.

We can generalize our method to study the 2^n to 2^{n-1} chaotic regions merging processes. If we consider $f^N(x)$ with $N = 2^{n-1}$, then the $2^n \to 2^{n-1}$ transition in f is a $2 \to 1$ transition in f^N. Defining

$$F(x) \equiv f^{2N}(x) = f^{(2n)}(x) , \tag{3.3}$$

we find that the condition for 2^n to 2^{n-1} transition can also be written as Eq. (3.2) with $F(x)$ given by (3.3). The set of λ_n for $2^n \to 2^{n-1}$ transition based on the simple iteration equation $x_{m+1} = \lambda x_m(1 - x_m)$ is listed in Table I.

2. 3 to 1 chaotic transition. Next, we consider the $3 \to 1$ transition. Refer to Figs. 6 and 9 and define three regions: I is (A, B), II is (C, D), and III is (F, G). It is easy to see that the mechanism described above cannot work. In Fig. 6 we find that the three regions are mapped into each other according to $\text{I} \to \text{II} \to \text{III} \to \text{I}$. Let us assume (falsely) that the first mechanism does occur. As these three regions start to overlap in a manner similar to that shown in Figs. 4 and 5, their intersections $\text{I} \cap \text{II}$, $\text{II} \cap \text{III}$, $\text{III} \cap \text{I}$ must map into each other to form a three cycle. Since regions I and III do not intersect, this scheme is not possible. Hence, only the second mechanism described in Figs. 6–9, is allowed.

In a typical three-region chaotic map, Fig. 6, the boundary points and the peak position $x = P$ are mapped according to

$$f\colon\ P \to G \to A \to C \to F \to B \to D \to H ,$$

where H is inside FG. For a singly peaked $f(x)$, folding can only occur around the peak $x = P$. In

TABLE I. Parameter λ_n for $2^n \to 2^{n-1}$ chaotic transition for the iteration $x_{m+1} = \lambda x_m(1 - x_m)$.

n	Transition parameter λ_n
1	3.678 573 510 428 322
2	3.592 572 184 106 979
3	3.574 804 938 759 208
4	3.570 985 940 341 615
5	3.570 168 472 496 377
6	3.569 993 388 559 135
7	3.569 955 891 325 221

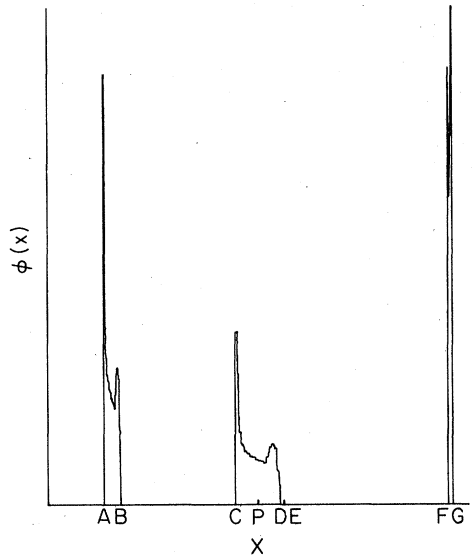

FIG. 6. Chaotic three cycle $\lambda = 3.856$.

terms of regions, we find that region I is mapped onto region II, region II after folding is mapped onto region III, and region III is mapped back onto region I.

There are two mechanisms for removing points from the gaps *BC* and *DF*. The first mechanism is through folding and mapping: Point *C* is folded onto point *E* (i.e., *E* also maps onto *F*, see Fig. 9) and the segment *DE* is thus mapped into the interior of *FG*. The line segment *DE* serves as a "drain" to the gap *BC* through which the points in the gap may escape. The remaining points in *BC* are mapped into *EF*. Upon a further iteration, *EF* maps into *BF*, which contains both the gaps *BC*, *DF*, and region II. Of course, all points which map into II are removed from the gaps forever. This serves as an alternative "sink" for removing points from the gaps.

As λ changes, we may encounter the situation where *D* and *E* coincide. Then, the drain *DE* is sealed, but the other drain still works. Hence, we still have two gaps and three separate regions. However, as λ increases further, the locations of *D* and *E* are interchanged. The sink now becomes a source, and points in region II can map into the gaps via the opening at *ED* (see Fig. 9). Of course, we still have the other drain to remove points from the gaps. The combined effect gives rise to a finite distribution in the gaps which represents the equilibrium distribution between the source and the sink just as in the case of a flooded basement. Since the seepage is controlled by the size of the gate, we expect that the value of ϕ inside the gaps increases continuously from zero with the increas-

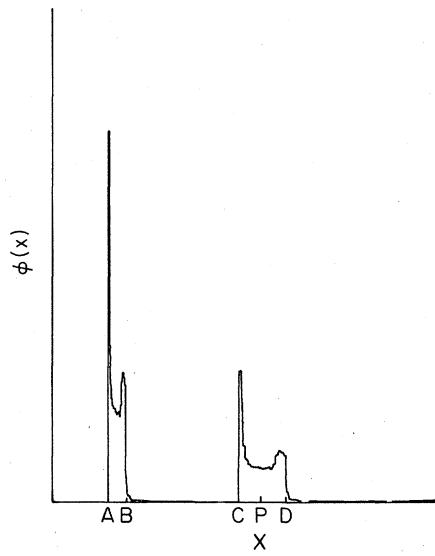

FIG. 7. At transition to single region $\lambda = 3.857$.

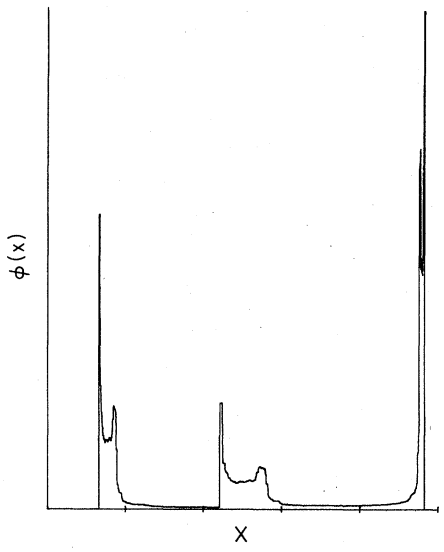

FIG. 8. Past transition to single region $\lambda = 3.858$.

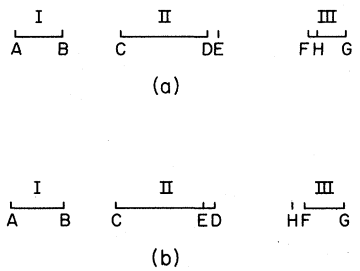

FIG. 9. (a) The ordering of the points discussed in the text for a chaotic three cycle. (b) The new order after the transition to a one cycle.

ing seepage. Figures 6—8 give actual graphical representations of ϕ in the neighborhood of a $3 \to 1$ transition.

Now, let us determine the condition for the $3 \to 1$ chaotic transition. As we have mentioned earlier, the $3 \to 1$ transition occurs when points D and E coincide. Since D is $f^6(P)$, and since point E maps into $F \equiv f^4(P)$, the condition for D and E to coincide is for $f(D) = f(E) = F$. This then implies

$$f^7(P) = f^4(P) . \tag{3.4}$$

Note that the points B, D, F form an unstable three cycle at the transition. In terms of $F(x) \equiv f^3(x)$, we can rewrite the above equation as the universal equation

$$F^3(P) = F^2(P) \neq F(P) . \tag{3.5}$$

Even though the $2 \to 1$ and $3 \to 1$ chaotic transitions arise from different mechanisms, they obey the same universal equation. The only difference is in the definition of F: F is f^2 for the $2 \to 1$ transition, and is f^3 for the $3 \to 1$ transition. We can generalize the above result to an arbitrary transition. For $f = \lambda x(1-x)$, the $3 \to 1$ chaotic transition occurs at

$$\lambda = 3.856\,800\,652\,477\,765\ldots .$$

3. Universal behavior. We now discuss the universality of the 2^n to 2^{n-1} transitions. In Table I, we see that as $n \to \infty$, λ_n approaches the infinite two-cycle bifurcation point $\lambda_\infty = 3.569\,945\,671\ldots$ from above. In fact, λ_n satisfies the asymptotic behavior

$$\lambda_n = \lambda_\infty + \frac{A}{\delta^n} \tag{3.6}$$

with

$$A = 0.494\,454\ldots$$

and

$$\delta = 4.669\,201\,609\ldots$$

is a universal constant introduced by Feigenbaum.[2] For $n \geq 6$, the agreement between the asymptotic formula and the true transition value is better than one part in 10^9. This asymptotic behavior follows from the renormalization group structure of the higher-order iterations as studied by Feigenbaum.[2] Indeed, if we consider the behavior of $F(x) \equiv f^{2^N}(x)$ at the $2N \to N$ transition in the neighborhood of $x = P$ and express the result in terms of the scaled variables

$$y \equiv \frac{x - F^2(P)}{F(P) - F^2(P)} ,$$
$$G_N(y) \equiv \frac{F(x) - F^2(P)}{F(P) - F^2(P)} , \tag{3.7}$$

we arrive at an invariant function $G(y)$ at large N. This invariant function G is a linear combination of the invariant functions g and h introduced by Feigenbaum.[2] Note that $G(0) = G(1) = 0$, and $G(1/2) = 1$. The invariant function $G(y)$ is shown in Fig. 10.

IV. FOLDING AND THE LYAPUNOV EXPONENT

A useful measure of the degree of mixing of a dynamical system is provided by the Lyapunov exponent. For a one-dimensional chaotic system, the Lyapunov exponent is simply related to the folding phenomena. We consider a simple one-dimensional mapping

$$x_{n+1} = f(x_n) . \tag{4.1}$$

The chaotic region is characterized by the fact that the separation of two neighboring points (x_n, y_n) will increase exponentially as we iterate (4.1) a large number of times. For an infinitismal separation, we refer to the average logarithmic increment defined by

$$\mu \equiv \lim_{n\to\infty} \frac{1}{n} \lim_{x_0 \to y_0} \ln \frac{|x_n - y_n|}{|x_0 - y_0|} = \lim_{n\to\infty} \frac{1}{n} \left(\sum_{i=0}^{n-1} \ln |f'(x_i)| \right) \tag{4.2}$$

as the Lyapunov exponent. The exponent μ is positive ($\mu > 0$) in the chaotic region. Let us start from a small neighborhood. After many iterations, the neighborhood will enlarge and eventually cover a compact space. Further iterations will map this compact space into itself. It is known that there exists a density function $\phi(x)$ such that $\phi(x)dx$ provides the probability measure for finding an arbitrary point inside the region dx after many iterations of Eq. (4.1). The probability function $\phi(x)$ is invariant under the iteration and hence is the eigenfunction with unit eigenvalue of the linear equation

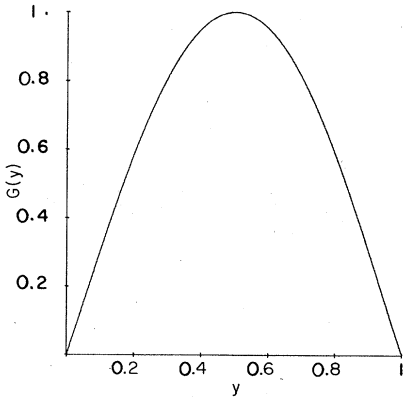

FIG. 10. The universal function $G(y)$.

$$\int K(x,y)\phi(y)dy = \phi(x)\,, \tag{4.3}$$

where

$$K(x,y) \equiv \delta[x - f(y)]\,. \tag{4.4}$$

We have learned from Lemma 3 of Sec. II that the support of ϕ may consist of N disjoint regions. The iteration of $K(x,y)$ [or (4.1)] will map points from one region to another, and bring the point back to the original region after N iterations. Thus, if we consider the iteration defined by

$$x_{n+1} = F(x_n)\,, \tag{4.5}$$

with

$$F(x) \equiv f^N(x) \equiv f(f^{N-1}(x))\,, \tag{4.6}$$

we encounter iterations which map a region back onto itself. Since the Lyapunov exponent μ associated with f is related to the exponent μ_N associated with F via

$$\mu = \frac{1}{N}\mu_N, \tag{4.7}$$

we only need to consider F and μ_N involving simpler mappings. A typical distribution function is shown in Fig. 11. Let AB be a region which maps into itself under F. The end point B is mapped onto point A, end point A and an interior point D are both mapped onto E $[F(A) = F(D) = E]$, and point P is mapped onto point B. This mapping may be achieved by folding PD on PA and then stretching BP to the original length AB (see Fig. 12). For more complicated mappings, it may be necessary to fold the line segment more than once. All the

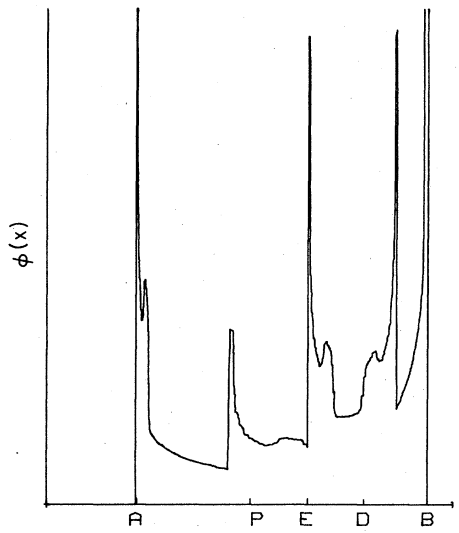

FIG. 11. Illustration of overlapping. Density function $\phi(x)$ for $\lambda = 3.75$.

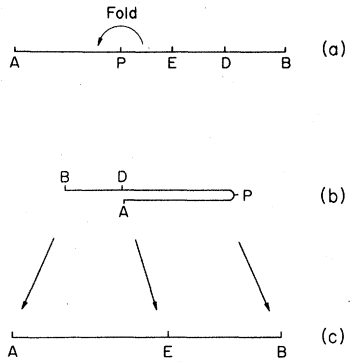

FIG. 12. Mapping involved in a chaotic one region: (a) Folding of AB about point P gives (b). Stretching BP completes the mapping shown in (c).

points in segment AE come from BD and the mapping is 1 to 1. We shall call this segment AE as nonoverlapping. The points in segment EB come from both AP and PD and the mapping is 2 to 1. We call this segment EB as overlapping.

We denote the density function ϕ within segments AP, PD, and DB as $\phi_{AP}(x)$, $\phi_{PD}(x)$, and $\phi_{DB}(x)$, respectively, obeying

$$\phi_{AP}(x) = \begin{cases} \phi(x), & \text{for } x \in (AP) \\ 0, & x \text{ outside } (AP) \end{cases} \tag{4.8}$$

etc. Then, we have

$$K^N \phi_{DB} = \phi_{AE}\,, \tag{4.9}$$

$$K^N \phi_{AP} \equiv (\phi_1)_{EB}\,, \tag{4.10}$$

$$K^N \phi_{PD} \equiv (\phi_2)_{EB}\,, \tag{4.11}$$

with

$$\phi_{EB} = (\phi_1)_{EB} + (\phi_2)_{EB}\,. \tag{4.12}$$

Equations (4.10) and (4.11) may be taken as the definitions of ϕ_1 and ϕ_2. In the following, we shall express the Lyapunov exponent as a function of ϕ, ϕ_1, and ϕ_2. The ϕ_1 and ϕ_2 for the ϕ of Fig. 11 are shown in Figs. 13 and 14.

It is more convenient to denote the separation of two neighboring points as $\phi(x)dx$ rather than as dx. To understand the definition of m using ϕ, consider a particular point x_1 and its neighborhood dx_1. Map it a sufficient number of times N such that it returns to its original neighborhood. If the new length is $d\bar{x}_1$, the magnification is

$$m \equiv \left(\frac{d\bar{x}_1}{dx_1}\right)^{1/N} = \left(\frac{\phi(x_2)dx_2}{\phi(x_1)dx_1}\,\frac{\phi(x_3)dx_3}{\phi(x_2)dx_2} \cdots \frac{\phi(x_1)d\bar{x}_1}{\phi(x_N)dx_N}\right)^{1/N}.$$

The enlargement and reduction due to the extra factor $\phi(x)$ cancels and we have the same overall magnification factor. The advantage of introducing this modified magnification factor is that the magnification factor is always one in the nonoverlap-

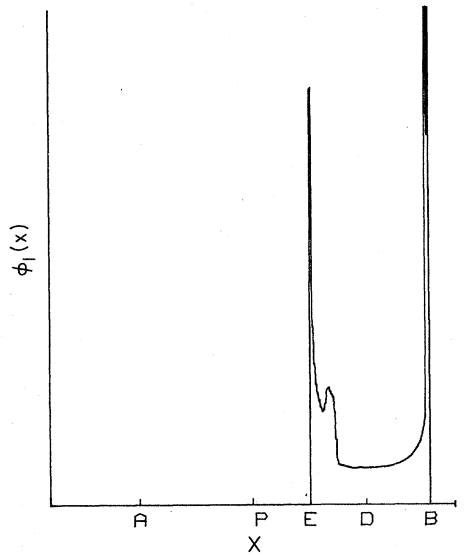

FIG. 13. Density function ϕ_1 (see text).

ping region due to the conservation of the probability under the mapping $x = F(y)$, giving

$$\phi(x)dx = \phi(y)dy \tag{4.13}$$

or

$$m \equiv \frac{\phi(x)dx}{\phi(y)dy} = 1 . \tag{4.14}$$

However, in the overlapping region, x can come from two or more different points, such as y_1 and y_2,

$$x = F(y_1) = F(y_2) \tag{4.15}$$

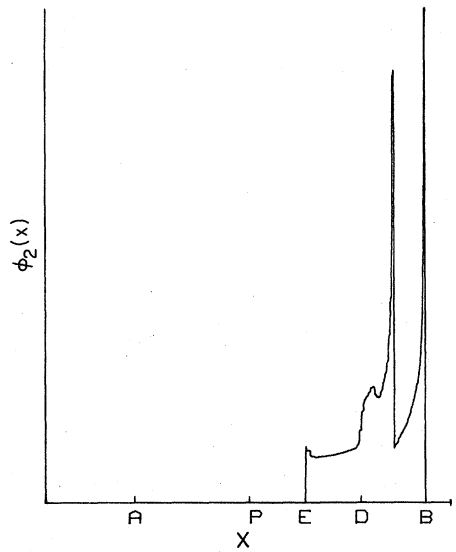

FIG. 14. Density function ϕ_2 (see text).

with

$$\phi_1(x)dx = \phi(y_1)dy_1 , \tag{4.16}$$

$$\phi_2(x)dx = \phi(y_2)dy_2 . \tag{4.17}$$

The magnification factors due to the mappings $y_1 \to x$ and $y_2 \to x$ are no longer one, and are given by

$$m(y_1) \equiv \frac{\phi(x)dx}{\phi(y_1)dy_1} = \frac{\phi(x)}{\phi_1(x)} , \tag{4.18}$$

$$m(y_2) \equiv \frac{\phi(x)dx}{\phi(y_2)dy_2} = \frac{\phi(x)}{\phi_2(x)} . \tag{4.19}$$

The geometrical average of the magnification factor m approaches

$$\bar{m} \equiv \lim_{n\to\infty} \left(\prod_i m(y_i) \right)^{1/n} ,$$

and the Lyapunov exponent becomes

$$\mu_N \equiv \ln\bar{m} = \lim_{n\to\infty} \frac{1}{n} \sum_i \ln m(y_i) . \tag{4.20}$$

To compute the limiting average magnification, we note that the weighting factor at any point y is proportional to its density $\phi(y)dy$. Thus, we can replace $\sum_i$ in (4.20) by an integral over $\phi(y)dy$ and n by $\int dy\, \phi(y)$, giving

$$\ln\bar{m} = \frac{\int_{AB} dy\, \phi(y) \ln m(y)}{\int_{AB} dy\, \phi(y)} .$$

In the numerator of the above equation, we can separate the y integration into three regions: Region DB which maps into the nonoverlapping region (AE) of x gives no contribution since $\ln m = 0$. The other y's are separated into y_1 and y_2 regions (AP and PD), and they both map into the overlapping region (EB) of x. The Lyapunov exponent becomes

$$\mu_N \equiv \ln\bar{m} = \frac{\int dy_1 \phi(y_1) \ln m(y_1) + \int dy_2 \phi(y_2) \ln m(y_2)}{\int_{AB} dy\, \phi(y)} .$$

The expression has a nicer form when expressed in terms of x. Using

$$\phi(y_k)dy_k = \phi_k(x)dx ,$$

$$m(y_k) = \frac{\phi(x)}{\phi_k(x)}, \quad (k = 1, 2)$$

we finally obtain

$$\mu_N \equiv \ln\bar{m} = \frac{\int_{EB} dx \left(\phi_1(x)\ln\frac{\phi(x)}{\phi_1(x)} + \phi_2(x)\ln\frac{\phi(x)}{\phi_2(x)}\right)}{\int_{AB} dx\,\phi(x)}$$

$$= \frac{\int_{EB} dx\,\phi(x)\left(\frac{\phi_1(x)}{\phi(x)}\ln\frac{\phi(x)}{\phi_1(x)} + \frac{\phi_2(x)}{\phi(x)}\ln\frac{\phi(x)}{\phi_2(x)}\right)}{\int_{AB} dx\,\phi(x)}. \tag{4.21}$$

The expression in the last large parenthesis of the numerator of (4.21) has the form of an entropy associated with the mixing of two independent statistical systems. We can generalize Eq. (4.21) trivially to include the folding of three or more regions.

For the folding of two regions, we introduce an overlapping factor r by

$$r(x) \equiv \left(\frac{\phi_1(x)}{\phi(x)}\ln\frac{\phi(x)}{\phi_1(x)} + \frac{\phi_2(x)}{\phi(x)}\ln\frac{\phi(x)}{\phi_2(x)}\right)\frac{1}{\ln 2}. \tag{4.22}$$

It is easy to see that $r=0$ if either ϕ_1/ϕ or ϕ_2/ϕ is zero, and r has a maximum, $r_{\max}=1$, at $\phi_1/\phi = \phi_2/\phi = \frac{1}{2}$. In terms of r and ϕ, we have

$$\mu_N = \int_{EB} dx\,\phi(x) r(x) \ln 2 \Big/ \int_{AB} dx\,\phi(x). \tag{4.23}$$

To compute μ_N (or μ), we need detailed information about ϕ_1, ϕ_2, and ϕ as functions of x. However, we can set a rather good upper bound on μ_N if we know the integrals of ϕ_1 and ϕ_2 in the overlapping regions. Let

$$M_1 \equiv \int_{EB} dx\,\phi_1(x), \quad M_2 = \int_{EB} dx\,\phi_2(x), \tag{4.24}$$

and

$$M \equiv \int_{AB} dx\,\phi(x). \tag{4.25}$$

we then define a mean overlapping factor as

$$R \equiv \frac{M_1}{M_1+M_2}\ln\frac{M_1+M_2}{M_1} + \frac{M_2}{M_1+M_2}\ln\frac{M_1+M_2}{M_2}. \tag{4.26}$$

One can show that

$$\mu_N \leq \frac{(M_1+M_2)}{M} R \ln 2. \tag{4.27}$$

For the particular coupling leading to the distribution functions of Figs. 9–11, we obtain $\mu = 0.36$ and the upper bound would give $\mu \leq 0.42$.

We have studied numerically the magnification factor and the Lyapunov exponent for the universal function G defined via Eq. (3.7) by sampling 300 000 iterations under G. The average magnification m_G, the Lyapunov exponent μ_G, and the average overlapping factor R_G are

$$m_G = 1.9872,$$

$$\mu_G = \ln m_G = 0.6867,$$

and

$$R_G = 0.9907,$$

respectively. The large magnification ($m \simeq 2$) and overlapping factor ($R \simeq 1$) are not surprising. Numerically, the universal function $G(y)$ is very close to the quadratic function $f(y) = 4y(1-y)$. The eigenfunction corresponding to the latter mapping is $\phi = 1/[x(1-x)]^{1/2}$. The iteration of $f(y)$ gives rise to the maximal magnification and overlapping factor $m=2$, $\mu = \ln 2$, and $R=1$, exactly.

Knowing the Lyapunov exponent μ_G for $G(y)$, we can compute the Lyapunov exponent $\mu(\lambda)$ for the original $f(x)$ at the $2N \to N$ transition point for large N. In particular, for the $2^n \to 2^{n-1}$ transition at large n, we have

$$\mu(\lambda_n) = 2^{-n}\mu_G. \tag{4.28}$$

Using the asymptotic formula Eq. (3.6), we obtain

$$2^{-n} = \left(\frac{\lambda_n - \lambda_\infty}{A}\right)^t \tag{4.29}$$

with

$$t = \frac{\ln 2}{\ln\delta} = 0.449\,806\,967. \tag{4.30}$$

Hence, we have

$$\mu(\lambda_n) = 0.6867\left(\frac{\lambda_n - \lambda_\infty}{A}\right)^t. \tag{4.31}$$

The $(\lambda - \lambda_\infty)$ power dependence has been recently obtained by Huberman and Rudnick.[3] We are also able to determine the prefactor in addition to the power dependence at these transition points.

V. BEHAVIOR OF EIGENVALUES NEAR THE CHAOTIC TRANSITIONS

We learned from Sec. II that there are two eigenvalues $\eta = \pm 1$ with $|\eta| = 1$ in the chaotic two-region. On the other hand, there is only one eigenvalue $\eta = 1$ with $|\eta| = 1$ in the chaotic one region. Thus, when the system makes a 2 to 1 chaotic transition, the $\eta = -1$ eigenvalue becomes an eigenvalue of $|\eta| < 1$.

In the chaotic two region, the eigenfunction ϕ_0 of $\eta = 1$ is real and positive. The support of ϕ_0 contains two separate regions I and II as in Fig. 4. The eigenfunction ϕ_1 associated with $\eta = -1$ also has the same support. We may choose ϕ_1 as

$$\phi_1 = \begin{cases} \phi_0, & \text{in region I} \\ -\phi_0, & \text{in region II.} \end{cases} \tag{5.1}$$

However, as one enters the chaotic one region, the previous two regions I and II overlap (see Fig. 5). To the first approximation, ϕ_0 in the overlapping region may be viewed as the sum of ϕ_0's in I and II, while ϕ_1 in the overlapping region is the difference. The interference of ϕ's in the overlapping region is responsible for reducing $|\eta|$ to less than 1. To understand qualitatively how η behaves near the transition, we consider the expression

$$\int dx\,dy\,K(x,y)\phi_0(y)\left(\frac{\phi(x)}{\phi_0(x)}+\frac{\phi(y)}{\phi_0(y)}\right)^2 = (2+2\eta)\int dx\,\frac{|\phi(x)|^2}{\phi_0(x)}, \tag{5.2}$$

which implies

$$1+\eta = \frac{\int dx\,dy\,K(x,y)\phi_0(y)\left(\frac{\phi(x)}{\phi_0(x)}+\frac{\phi(y)}{\phi_0(y)}\right)^2}{2\int dx\frac{|\phi(x)|^2}{\phi_0(x)}}. \tag{5.3}$$

In (5.2) and (5.3), we have made use of the fact that η and ϕ are real. When λ is smaller than the transition eigenvalue λ_1, the regions I and II are disjoint. In this case, we have

$$K(x,y)\left(\frac{\phi(x)}{\phi_0(x)}+\frac{\phi(y)}{\phi_0(y)}\right)^2 = 0 \tag{5.4}$$

and hence

$$1+\eta = 0, \quad \lambda < \lambda_1. \tag{5.5}$$

When $\lambda > \lambda_1$ regions I and II overlap and the left-hand side (lhs) of Eq. (5.2) no longer vanishes. We find that

$$\left(\frac{\phi(x)}{\phi_0(x)}+\frac{\phi(x)}{\phi_0(y)}\right)^2 = 0(1) \tag{5.6}$$

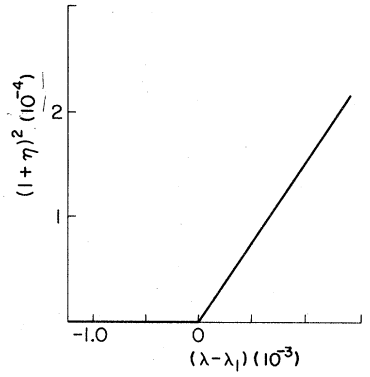

FIG. 15. $(1+\eta)^2$ as a function of $\lambda-\lambda_1$ near the 2 to 1 chaotic transition $\lambda = 3.6786$.

for x in the overlapping region. One can show that the only important region of integration in the lhs of Eq. (5.2) is for x in the overlapping region. With x in the overlapping region (OR), we may have a crude estimate of $1+\eta$ as,

$$1+\eta \simeq \frac{0(1)\int_{OR} dx \int dy K(x,y)\phi_0(y)}{\int dx\,\phi_0(x)} = \frac{0(1)\int_{OR} dx\,\phi_0(x)}{\int dx\,\phi_0(x)}. \tag{5.7}$$

In deriving (5.7), we have also approximated $|\phi(x)|^2/\phi_0(x)$ in the denominator of Eq. (5.3) by ϕ_0. Equation (5.7) indicates that $1+\eta$ is proportional to the integrated density of ϕ_0 in the overlapping region. Note that the size of the overlapping region δ is proportional to $\delta\lambda \equiv \lambda - \lambda_1$ and that $\phi_0(x)$ is dominated by square-root singularities $1/(|x-x_i|)^{1/2}$, in the overlapping region. Hence, we have

$$1+\eta = \begin{cases} \propto \int_0 \frac{dx}{(|x-x_i|)^{1/2}} \propto \sqrt{\delta\lambda}, & \lambda > \lambda_1 \\ 0, & \lambda < \lambda_1. \end{cases} \tag{5.8}$$

The constant of proportionality depends on the detailed structure of $\phi_0(x)$ and on the rate of change of the overlapping region. However, we know that in the vicinity of $\lambda = \lambda_1$, $(1+\eta)^2$ is zero for $\lambda < \lambda_1$ and increases linearly with λ for $\lambda > \lambda_1$. In Fig. 15, we plot $(1+\eta)^2$ as a function of λ. The transition and the linear dependence in λ are indeed verified numerically.

We may generalize the method to study the change of eigenvalue η near a $3 \to 1$ chaotic transition. In the chaotic three region, the eigenvalues with $|\eta| = 1$ are 1, $\eta_0 \equiv \frac{1}{2}(-1+\sqrt{3}i)$, and η_0^*. The $\phi_0(\eta = 1)$ state contains three separate pieces I, II, and III as shown in Fig. 6. The η_0 (or η_0^*) state is obtained from ϕ_0 by assigning three different phases $1, \eta_0, \eta_0^*$ $(1, \eta_0^*, \eta_0)$ to regions I, II, and III. In the chaotic one region, only the eigenvalue $\eta = 1$ remains to be of magnitude 1. The other two eigenvalues η, η^* now have magnitude less than one (i.e., $|\eta| < 1$). We can also study the rate of $|\eta|$ approaching one near the transition region $\lambda = \lambda_1$. In analogy to Eq. (5.3), we have

$$2-\eta_0^*\eta-\eta_0\eta^* = \frac{\int dx\,dy\,K(x,y)\phi_0(y)\left|\frac{\phi(x)}{\phi_0(x)}-\eta_0^*\frac{\phi(y)}{\phi_0(y)}\right|^2}{\int dx\frac{|\phi(x)|^2}{\phi_0(x)}}. \tag{5.9}$$

For $\lambda < \lambda_1$, we are in the chaotic three region and both sides of Eq. (5.9) vanish identically. For $\lambda > \lambda_1$ we are in the single chaotic region. As we have shown in Sec. IV, the gaps between regions

I and II and regions II and III develop nonvanishing ϕ_0. The magnitude of ϕ_0 in the gaps is proportional to the incoming flux (source) via the gate DE. The magnitude of the source is given by

$$\text{Source} = \int_{\text{gate}} dx\, \phi_0(x) \propto \sqrt{\delta\lambda} \tag{5.10}$$

with $\delta\lambda \equiv \lambda - \lambda_1$. Thus, $\phi_0(x)$ in the gap region is also proportional to $\sqrt{\delta\lambda}$. Now, we look at the numerator on the right-hand side (rhs) of Eq. (5.9). The important contribution to the numerator comes from the integration region where y is in the gap region DF. The requirement of $K(x,y) \neq 0$ implies that x is in the gaps or in region II. Then, the phase correlation factor is

$$\left| \frac{\phi(x)}{\phi_0(x)} - \eta_0^* \frac{\phi(y)}{\phi_0(y)} \right|^2 = 0(1) .$$

We then have the estimate

$$2 - \eta_0^*\eta - \eta_0\eta^* \simeq 0(1) \frac{\int dx \int_{\text{gap}} dy\, K(x,y)\phi_0(y)}{\int dx \phi_0(x)}$$

$$= 0(1) \int_{\text{gap}} dy\, \phi_0(y) \Big/ \int dx\, \phi_0(x) \propto \sqrt{\delta\lambda} . \tag{5.11}$$

Near $\eta = \eta_0$, we can rewrite the lhs of (5.11) as

$$2 - \eta_0^*\eta - \eta_0\eta^* = 1 - \eta\eta^* + |\eta_0 - \eta|^2$$

$$= 2(1 - |\eta|) + |\eta_0 - \eta|^2 - (1 - |\eta|)^2 . \tag{5.12}$$

Ignoring terms second order in smallness, we have

$$1 - |\eta| = \begin{cases} \propto \sqrt{\delta\lambda}, & \lambda > \lambda_1 \\ 0, & \lambda < \lambda_1 \end{cases} \tag{5.13}$$

as before. We have studied $(1 - |\eta|)^2$ as a function of λ numerically and indeed observed the above dependence.

ACKNOWLEDGMENTS

We wish to thank Professor A. Jackson and Professor R. L. Schult for stimulating discussions. This work was supported in part by the National Science Foundation under Grant No. NSF PHY 79-00272, and by the Office of Naval Research under Contract No. N00014-80-C-0840.

APPENDIX A: NUMERICAL METHOD

To find the eigenvalues and eigenfunctions of the operator K given in Eq. (2.7) we used a relatively straightforward, but possibly inefficient method. Basis functions for the space were chosen to be

$$f_n(x) = \begin{cases} 1, & x_n < x < x_{n+1} \\ 0, & \text{otherwise} \end{cases} \tag{A1}$$

where the x_n were a prescribed set of points on $(0,1)$. K is then expanded in this basis set. The problem that arises is that a large matrix is needed (on the order of 1000×1000) for reasonable accuracy. The reason for this is essentially that discussed in Sec. II; that is, the width of K controls the number of bifurcations that are possible. A better choice of basis functions might alleviate this problem somewhat. Fortunately, most of the elements of K are zero, in fact, the number of nonzero elements is about twice the linear dimension of K.

We are now faced with finding the eigenvalues and eigenvectors of a large sparse matrix. Since we are only interested in the largest eigenvalues it is appropriate to use an iterative technique. To find the equilibrium-density distribution straightforward iteration of the discretized version of Eq. (A1) works fairly well, the only complication being in sorting out ϕ_0 from the other eigenvectors with eigenvalues of modulus 1. Our pictures of ϕ_0 used this method.

The eigenvalue (and associated eigenvector) problem is more complicated. We used a version of the Lanczos method. See, for example, Wilkinson[7] for a complete description. The idea is to start from an arbitrary left state L_1 and an arbitrary right state R_1 and iterate:

$$KR_1 = a_1R_1 + b_2R_2 ,$$

$$L_1K = a_1L_1 + s_2b_2L_2 . \tag{A2}$$

At the nth step we have,

$$KR_n = a_nR_n + b_nR_{n+1} + s_nb_nR_{n-1} ,$$

$$L_nK = a_nL_n + s_{n+1}b_{n+1}L_{n+1} + b_nL_{n-1} . \tag{A3}$$

The newly generated R_{n+1} is chosen to be orthogonal to all previous generated L_n; similarly for L. We choose $\langle L_n | R_n \rangle = 1$. This completely determines the coefficients a_n and b_n. S_n is just a sign ± 1. In this scheme it is easily seen that a tridiagonal matrix for K is generated. We typically used a 30×30 matrix. Actually it is important to use several sizes say 26–30 and only the stable eigenvalues are relevant. That is, new eigenvalues are introduced at each stage and they typically change as the matrix size is increased. The eigenvectors can easily be calculated this way, but we have not actually done that. The absolute accuracy of predicting transitions was of the order of several percent, but the relative accuracy is much better. This enables us to compute the scaling of eigenvalues near transitions quite accurately.

APPENDIX B: ALTERNATIVE PROOF OF LEMMA 3

In this appendix we present an alternative proof of Lemma 3 that is valid for any number of dimensions. We start with a proposition that is proved in Ref. 6. It states that under fairly general conditions an operator satisfying Eqs. (2.2) and (2.3) has a cyclic peripheral spectrum. That is to say that if there are N eigenvalues with absolute value one, those eigenvalues are all of the Nth roots of unity. If there is a degeneracy the spectrum must be divided into classes satisfying the above condition. We will assume that there is no degeneracy. Thus we are given

$$\phi_0, \phi_1, \ldots, \phi_{N-1},$$

such that

$$K\phi_j = \omega^j \phi_j,$$

with

$$\omega = e^{2\pi i/N}. \tag{B1}$$

From Lemma 2 we know that we can choose

$$\phi_j(x) = e^{i\theta_j(x)}\phi_0(x), \quad j = 1, \ldots, N-1. \tag{B2}$$

We further choose the phases such that at a particular point $x = a$ with $\phi_0(a) \neq 0$,

$$\theta_j(a) = 0, \quad j = 1, \ldots, N-1. \tag{B3}$$

We first prove a Lemma: If, for K, satisfying Eqs. (2.2) and (2.3) there exist $\psi_0, \ldots, \psi_{N-1}$ such that

$$\int K(x,y)\psi_j(y)dy = \psi_{j+1}(x) \tag{B4}$$

and

$$\psi_N(x) \equiv \psi_0(x),$$

then

$$\int K(x,y)\,|\psi_j(y)|\,dy = |\psi_{j+1}(x)|. \tag{B5}$$

Proof. Taking the absolute value of Eq. (B4), we obtain

$$\int K(x,y)\,|\psi_j(y)|\,dy \geq |\psi_{j+1}(x)|. \tag{B6}$$

Integrating Eq. (B6) gives the cyclic set of inequalities

$$\int |\psi_j(x)|\,dx \geq \int |\psi_{j+1}(x)|\,dx.$$

Because of the cylic nature the equality sign must hold, which implies Eq. (B5), except perhaps on a set of measured zero. Thus the Lemma is proved.

We now prove the important theorem which says that the support of the eigenfunctions consist of disjoint regions and the phases of each eigenfunction are constant within those regions.

Theorem. There exist N nonnegative functions $\chi_j(x)$ having disjoint support such that

$$K\chi_j = \chi_{j+1} \tag{B7}$$

and the χ_j serve as a basis for expansion of the eigenfunctions having modulus 1.

Proof. Construct

$$\chi_0 = \frac{1}{N}\,|1 + e^{i\theta_1} + \ldots + e^{i\theta_{N-1}}|\,\phi_0,$$

$$\chi_1 = \frac{1}{N}\,|1 + \omega e^{i\theta_1} + \omega^2 e^{i\theta_2} + \ldots\,|\,\phi_0,$$

$$\chi_2 = \frac{1}{N}\,|1 + \omega^2 e^{i\theta_1} + \omega^4 e^{i\theta_2} + \ldots\,|\,\phi_0,$$

$$\ldots$$

$$\chi_{N-1} = \frac{1}{N}\,|1 + \omega^{N-1} e^{i\theta_1} + \ldots\,|\,\phi_0.$$

It is trivial to verify from Eqs. (B1) and (B2) that without the absolute value signs, the χ_j satisfy Eq. (B4). From the above Lemma we see that they satisfy Eq. (B7). We further note that at $x = a$ where $\theta_j(a) = 0$,

$$\chi_0(a) = \phi_0 \neq 0,$$

$$\chi_j(a) = 0, \quad j \neq 0.$$

(This follows from the fact that the sum of the Nth roots of unity is zero.) Next construct

$$\xi_0 = (\chi_0 + \chi_1 + \ldots + \chi_{N-1}),$$

$$\xi_1 = \left(\chi_0 + \frac{1}{\omega}\chi_1 + \frac{1}{\omega^2}\chi_2 + \ldots\right), \tag{B8}$$

$$\xi_2 = \left(\chi_0 + \frac{1}{\omega^2}\chi_1 + \ldots\right),$$

etc. These functions satisfy

$$K\xi_j = \omega^j \xi_j$$

so we conclude that

$$\xi_j = C_j \phi_j.$$

Now at $x = a$ we have

$$\xi_j = \phi_0, \quad j = 0, 1, \ldots, N-1.$$

Thus

$$C_j = 1, \quad j = 0, \ldots, N-1.$$

Taking the absolute value of Eqs. (B8) we obtain

$$\chi_0+\chi_1+\ldots+\chi_{N-1}\equiv\phi_0=|\xi_j|,\quad j=1,\ldots,N-1.$$

Because the coefficients ω^j point in different directions in the complex plane, the functions χ_j must have disjoint support. Finally the construction of ξ_j demonstrate the constancy of their phases (ω^{-jk}) in the kth region.

[1]R. H. May, Nature 261, 459 (1976).
[2]M. J. Feigenbaum, J. Stat. Phys. 19, 25 (1978); 21, 669 (1979), Phys. Lett. 74A, 375 (1979).
[3]B. A. Huberman and J. Rudnick, Phys. Rev. Lett. 45, 154 (1980).
[4]J. Crutchfield and B. Huberman (unpublished).
[5]J. Crutchfield, D. Farmer, N. Packard, R. Shaw, G. Jones, and R. J. Donnely, Phys. Lett. 76A, 1 (1980).
[6]H. H. Schaefer, *Banach Lattices and Positive Operators* (Springer, Berlin, 1974), see Sec. (V.4).
[7]J. H. Wilkinson, *The Algebraic Eigenvalue Problem* (Clarendon, Oxford, 1965).